Research Article

Synthesis, identification and computational studies of novel Schiff bases *N*-(2,6-dibenzylidenecyclohexylidene)-*N*′-(2,4-dinitrophenyl) hydrazine derivatives

Md Mizanur Rahman Badal[1] · **Md Zakaria Hossain**[1] · **Md Maniruzzaman**[1] · **Mohammad Abu Yousuf**[1]

Received: 10 August 2020 / Accepted: 20 October 2020 / Published online: 28 October 2020

Abstract

Novel Schiff base of *N*-(2,6-dibenzylidenecyclohexylidene)-*N*′-(2,4-dinitrophenyl)hydrazine derivatives were synthesized by the condensation of 2,4-dinitrophenylhydrazine with substituted 2,6-dibenzylidenecyclohexanone. The synthesized compounds were characterized by UV-Visible, Fourier transform infrared, nuclear magnetic resonance and elemental analysis studies. Density functional theory was performed to predict structural geometries of compounds. The structures were optimized using B3LYP/6-311G+(2d,p) basis sets. The energies of HOMO and LUMO were found −6.23109 eV and −3.21595 eV for **4a**, −5.77287 eV and −2.95528 eV for **4b**, −5.28554 eV and −2.76835 eV for **4c** respectively. These results revealed the possibility of intramolecular charge transfer during excitation of the molecules. Other quantum chemical parameters of compound were also calculated.

Keywords Schiff base · Density functional theory · Bis-chalcones · Single point energy · Nonlinear structure

1 Introduction

A compound in which the C=O is replaced by a C=N is known as an imine or Schiff base. It was first discovered by a German chemist, Hugo Schiff [1]. Hydrazone is one kind of Schiff base and it is a class of organic compounds having the basic structure R1R2C=NNH- [2]. High physiological activity is the most important properties of hydrazones and is an important class of compounds containing an azomethine group (–NHN=C–) having two different nature of connected nitrogen atoms and a C=N double bond that is conjugated with a lone pair electron of the terminal nitrogen atom [3–5]. Extensive studies have revealed that the nitrogen atom of azomethine group having the lone pair of electrons in its sp^2 hybridized orbital is considered responsible the chemical and biological activities [6, 7]. Schiff base ligands are the important ligands in coordination chemistry owing to their ease of preparation, structural variety and polydenticity. These ligands show miscellaneous uses comprising electro-chemical behavior and biological field [8]. The metal complexes of Schiff base ligands are also promising features since the uses of Schiff base ligands enormously become widespread upon coordination with metal ions [9, 10]. The coordination mode adopted by hydrazone depends on various factors such as tautomerism, various reactions conditions, nature and number of the substituents on hydrazone skeleton and stability of the complex formed. The structural changes of the different segment attached to the hydrazine will affect the metal binding of the ligand and exhibit fascinating

---

Electronic supplementary material The online version of this article (https://doi.org/10.1007/s42452-020-03745-4) contains supplementary material, which is available to authorized users.

✉ Md Mizanur Rahman Badal, mizan@chem.kuet.ac.bd | [1]Department of Chemistry, Khulna University of Engineering & Technology, Khulna 9203, Bangladesh.

coordination modes with transition metal ions and formed different types of complexes [11, 12]. Membrane sensors based on Schiff bases also act as chelating ionophores in trace analysis for organic pollutants, metal ions and biological substances [13]. Particularly the 2,4-dinitrophenylhydrazones derivatives based Schiff bases have been shown to be potentially DNA-damaging and mutagenic agents [14]. In addition, the 2,4-dinitrophenylhydrazones derivatives exhibit good nonlinear optical (NLO) and crystalline properties [15, 16]. Owing to their significant applications, these compounds have attracted much attention to the researchers. But still, there are few reports based on both experimental and computational study of 2,4-dinitrophenylhydrazone derivatives based Schiff bases. Therefore, in order to obtain further information about 2,4-dinitrophenylhydrazone derivatives such as *N*-(2,6-dibenzylidenecyclohexylidene)-*N′*-(2,4-dinitrophenyl) hydrazine derivatives (Scheme 1), the compounds were synthesized and characterized by UV-Visible, Fourier transform infrared (FTIR), nuclear magnetic resonance (NMR) and elemental analysis studies. The structures were optimized by density functional theory (DFT) method. Furthermore, quantum chemical calculation, molecular orbital energy, mulliken charge and frontier orbital constitution were performed to divulge the energy of the examined compounds.

2 Results and discussion

Substituted bis-chalcone based hydrazones were synthesized by condensation of substituted bis-chalcones with hydrazine as previously shown in Scheme 1. The products were identified on the basis of UV-Visible, FTIR, NMR spectra and elemental analysis. The FTIR spectra of all compounds showed the characteristics stretching vibration of the NH group at 3263–3270 cm^{-1}. This band along with the C=N absorption band between 1612 and 1620 cm^{-1}, is a strong evidence for the presence of an azomethine group [17]. The C=C in conjugation with C=N and C=C stretching of phenyl showed at 1585–1590 cm^{-1}. Another important band at 1385–1392 cm^{-1} was attributed to stretching of C–NH. The substituted hydrazones were further examined by their ^{1}H NMR and ^{13}C NMR spectra in DMSO-d$_6$. The characteristics signals for the protons of NH- were observed δ = 11.5 ppm as well as aromatic protons in the region of δ from 7.22 to 8.79 ppm. The values are in good agreement with the literature values [17]. In ^{13}C NMR spectra, the significant signals are for azomethine carbon between δ from 143 and 150 ppm. This values are also similar as literature values [18].

3 Computational study

3.1 Geometry optimization

Optimized structures is the key materials to define its structural parameters. The examined compounds were optimized at DFT/6-311G+(2d,p) level of theory. Single point energies of the measured compounds were shown in Table 1.

Among the optimized structure, compound *N*-(2,6-(4-dimethylaminobenzylidene)-*N′*-(2,4-dinitrophenyl)

Table 1 Single point energies of the substituted *N*-(2,6-dibenzylidenecyclohexylidene)-*N′*-(2,4-dinitrophenyl)hydrazine in hartree

Basis set	4a	4b	4c
B3LYP/6-311G+(2d,p)	−2443.376300	−1753.248256	−1792.143341

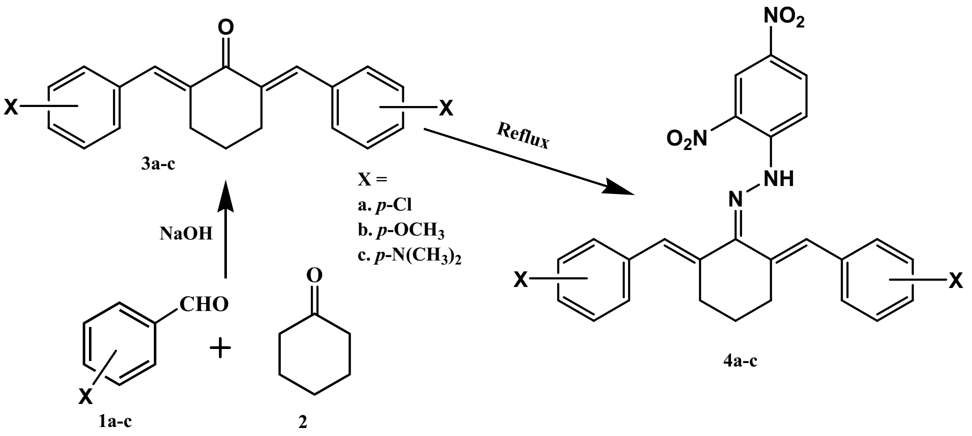

Scheme 1 Preparation of substituted *N*-(2,6-dibenzylidenecyclohexylidene)-*N′*-(2,4-dinitrophenyl)hydrazine

hydrazine by means of B3LYP/6-311G+(2d,p) basis set was shown in Fig. 1.

Rotational isomer of the examined compounds based on N–H group relative to NO_2 were also checked by the same method. It was found that the isomer where N–H and NO_2 on the same side are stable and forming intramolecular hydrogen bond with the bond distance 1.86 Å.

The structural parameters such as bond lengths, bond angles and dihedral angles of the examined compounds using DFT/6-311G+(2d,p) basis set given in Table 2**.** The C=N bond distance for all the substituted hydrazones are similar and the value is 1.2956 ± 0.002. The values are good agreement with the experimental reported values [19]. Both benzene rings are regular hexagons with C–C bond lengths (1.40 Å) somewhat in between the normal values for a single (1.54 Å) and a double (1.33 Å) bond [20]. For simplify the calculation, the compound has three phenyl rings as designated C8–C13 (PhI), C15–C20 (PhII), C15–C20 (PhIII) and cyclohexayl rings. Dihedral angles of a molecule provided information about planarity. Generally the values of dihedral angle is 0°, 180° or 360° showed planarity of a molecule. The calculated dihedral angles between these ring planes are as PhI/PhII = 52.12, PhII/PhIII = 8.92 and PhI/PhIII = 50.88. These results revealed that the rings are in out-of-plane. The bond angles of the optimized structures are also calculated. The C3 atom in cyclohexayl ring makes bond angles, C3–C2–C13 = 118.86 Å and C3–C4–C14 = 119.71 Å. The C26 atom in phenyl ring makes bond angles, C13–C26–C28 = 117.88 Å and C13–C26–C27 = 125.97 Å as well as C14–C16–C17 = 118.09 Å

Table 2 Selected bond lengths and dihedral angles of the substituted *N*-(2,6-dibenzylidenecyclohexylidene)-*N*′-(2,4-dinitrophenyl) hydrazine, **4a**–**c**

	Compounds		
	4a	**4b**	**4c**
Bond distances (Å)			
C23–N22	1.3510	1.3832	1.3564
N22–N21	1.3635	1.3623	1.3596
N21–C3	1.2976	1.2956	1.2938
C3–C2	1.4813	1.4827	1.4838
C2–C7	1.3514	1.3494	1.3480
C3–C4	1.4879	1.4901	1.4913
C4–C8	1.3468	1.3465	1.3479
Bond angle (°)			
C3–C2–C13	118.86	117.98	117.58
C3–C4–C14	119.71	119.11	118.75
C13–C26–C28	117.88	118.10	116.98
C13–C26–C27	125.97	126.12	125.58
C14–C16–C17	118.09	118.94	117.75
C14–C16–C18	125.90	126.14	124.85
Dihedral angle (°)			
N21–C3–C2–C7	−27.65	−28.10	−27.45
N21–C3–C4–C8	59.20	57.44	56.07
N22–N21–C3–C2	−179.52	−178.95	−179.28
N22–N21–C3–C4	−178.96	−178.52	−178.58

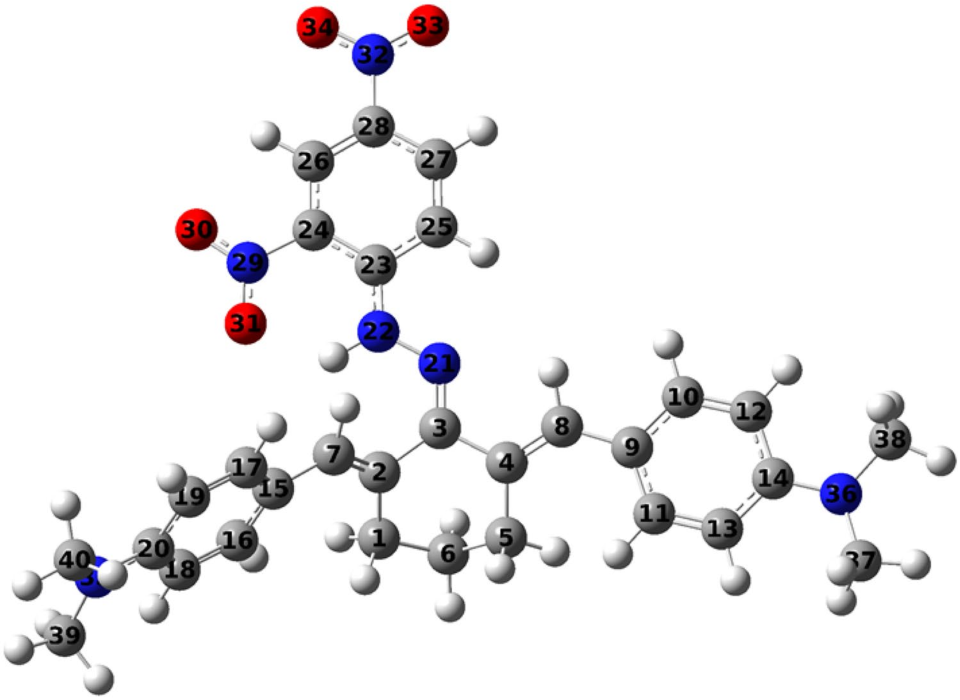

Fig. 1 Optimized structure of *N*-(2,6-(4-dimethylaminobenzylidene)-*N*′-(2,4-dinitrophenyl)hydrazine at DFT B3LYP/6-311G+(2d,p) level of theory

and C14–C16–C18 = 125.90 Å. All the bond angles are significantly deviated from trigonal planarity. The other Schiff base derivatives found similar results which shown in Table 2.

3.2 Vibrational and NMR studies

The IR spectra of the examined compounds calculated at the DFT/6-311G+(2d,p) level of theory and scaled by 0.9688 [21]. The calculated and the observed FTIR spectra showed good agreement that shown in Table 3.

Therefore, more trustworthy consignment of IR active modes of vibration can be performed by comparing experimental FTIR intensities with the computed wavenumbers. The sharp band for N–H stretching frequencies are found in the region of 3342 cm^{-1}.The C–H stretching vibrations of the aromatic are found in the frequency region of 3141, 3105 and 3028 cm^{-1}. Generally, in the aromatic system, stretching vibrations of C–H occur in variable intensity at 3093, 3075, 3030, and 3017 cm^{-1} [22]. The C–H stretching of aliphatic system is found in the region 2981–2891 cm^{-1}. The aromatic stretching of C–C occur at 1596–1592 cm^{-1}. The sharp band in the frequency of 1339–1314 cm^{-1} and 1157–1069 cm^{-1} are assigned as stretching vibration of C–N bond.

Table 3 Comparison of experimental FTIR spectra with calculated (scaled) IR spectra at DFT B3LYP/6-311G+(2d,p) level of theory

Subs.	Exp./FTIR (cm^{-1})	Cal./IR (cm^{-1})	Vibrational assignment
	3263	3342	ν_{NH}
	3095	3105	ν_{CH}
	2941, 2916	2981, 2951	ν_{CH}
4a	1612	1600	ν_{CN}
	1585	1596	ν_{CC}
	1508, 1490	1565, 1486	ν_{NO}
	1332, 1082	1314, 1069	ν_{CN}
	827	823	ν_{CCl}
	3269	3343	ν_{NH}
	3107	3141	ν_{CH}
	2931, 2835	2915, 2929	ν_{CH}
4b	1612	1596	ν_{CN}
	1585	1592	ν_{CC}
	1506, 1475	1562, 1496	ν_{NO}
	1249, 1130	1243, 1157	ν_{CN}
	1170	1166	ν_{CO}
	3271	3341	ν_{NH}
	3091	3028	ν_{CH}
	2931, 2835	2972, 2891	ν_{CH}
4c	1612	1603	ν_{CN}
	1602	1597	ν_{CC}
	1502, 1413	1507, 1401	ν_{NO}
	1327, 1305	1339, 1305	ν_{CN}

The nuclear shieldings (absolute values) are computed by gauge independent atomic orbital method (GIAO) with B3LYP/6-311G+(2d,p) level of theory. The calculated ^1H NMR for the examined compounds showed that the characteristics signals for the protons of NH are found between δ from 12.55 to 12.66 ppm. On the other hand for ^{13}C NMR signals for azomethine carbon between δ from 149.51 to 149.76 ppm. These values are in good agreement with the experimental results.

3.3 Electronic properties

Frontier molecular orbital (FMO) and molecular electrostatic potential (MEP) calculations of compounds are performed by DFT/B3LYP/6-311G+(2d,p) method. Since MEP maps show three-dimensional charge distribution of molecules, they provide information about electron acceptor as well as electron donor regions [23]. These regions are represented by different colors. On MEP map, red regions constitute negative potential areas, where blue color constitute positive potential areas and finally green color refers to zero potential areas. To estimate possible intermolecular and intramolecular hydrogen bonds as well as intermolecular charge transfer (ICT), these regions have to be focused. As the MEP map for the compounds **4a**–**4c** in Fig. 2 are examined, it could be seen that the highest negative and lowest negative regions line up according to the positioning of O and N atoms, respectively.

3.4 Frontier molecular orbitals

HOMO and LUMO molecular orbitals are the frontier orbitals and they show electron donor and electron acceptor ability of the molecule, respectively as presented by Parr and Nitti [24, 25]. The E_{HOMO} and E_{LUMO} energies correspond to ionization energy (I) and electron affinity (A), respectively.

As Fig. 3, it can be seen that HOMO is located in the whole region except for PhII ring and LUMO is located only in PhIII. Therefore it exposed that intramolecular charge transfer is predominantly happened during excitation of the molecules. The computed energies of HOMO and LUMO is −6.23109 eV and −3.21595 eV for **4a**, −5.77287 eV and −2.95528 eV for **4b**, −5.28554 eV and −2.76835 eV for **4c** respectively. Ionization potential is the energy absorbed as one electron is released from HOMO and its trend follows the decreasing order: **4a** > **4b** > **4c**, while electron affinity, which is the energy released when one electron is added to LUMO decreases in the order: **4a** > **4b** > **4c**. From these results it is concluded that **4a** absorbs high energy to becoming a cation and also

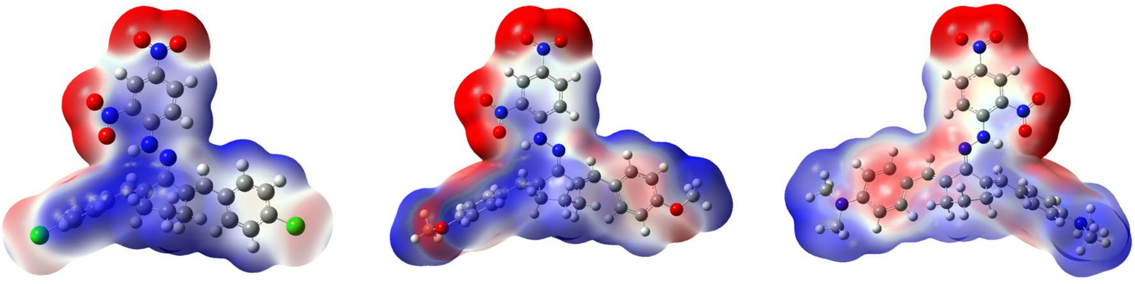
4a 4b 4c

Fig. 2 Molecular Electrostatic Potential (MEP) calculated at DFT B3LYP/6-311G+(2d,p) level of theory

Substituent	HOMO	LUMO
4a	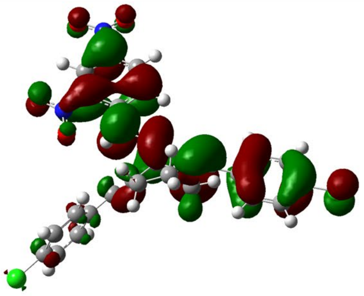	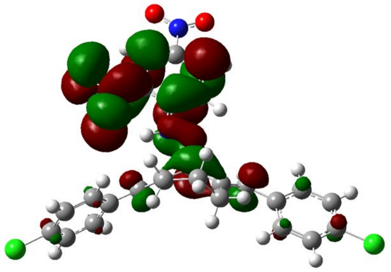
4b	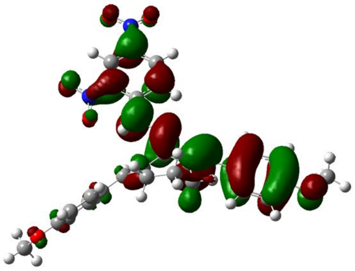	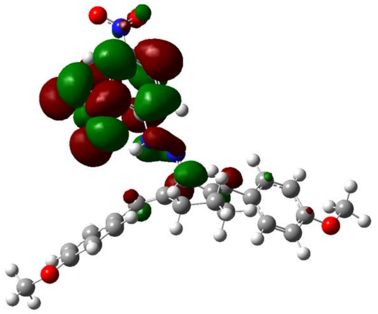
4c	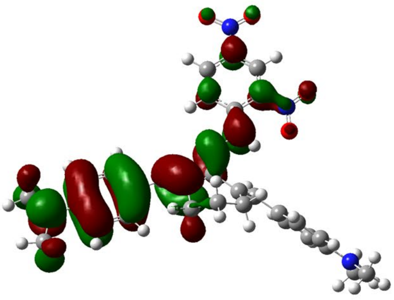	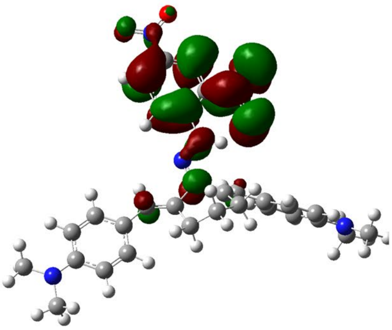

Fig. 3 HOMO and LUMO of substituted *N*-(2,6-dibenzylidenecyclohexylidene)-*N′*-(2,4-dinitrophenyl)hydrazine at B3LYP/6-311G+(2d,p) level of theory

releases high energy to becoming an anion in relation to the others in the group. According to quantum theory, the mixing of appropriate excited state wave functions with the ground state wave function changes the electron density of the chemical entity and the mixing coefficient is inversely proportional to the excitation energy between the ground and the excited state. So, the rigid molecule has a large HOMO–LUMO gap on the other hand a soft molecule has a small HOMO–LUMO gap. For considering chemical reactivity, soft molecules with a small gap in their electron density alter more easily and hence will be more reactive than hard molecule. For the studied schiff base derivatives, compound **4c** having small value of HOMO-LUMO gap indicates a soft molecule with high reactivity compared to the others.

Quantum chemical parameters such as chemical hardness (η) and softness (σ); chemical potential (μ) and electronegativity (χ); nucleophilicity (ε) and electrophilicity (ω) can be calculated using the following equations [26].

$$\chi = -\mu = (I + A)/2; \eta = (I - A)/2; \sigma = 1/\eta; \omega = \mu^2/2\eta = \chi^2/2\eta; \text{and } \varepsilon = 1/\omega$$

The values of **4a–4c** compounds are; $\chi = -\mu = 4.72$ eV, 4.36 eV, 4.03 eV; $\eta = 1/\sigma = 1.51$ eV, 1.41 eV, 1.26 eV and $\omega = 1/\varepsilon = 7.39$ eV, 6.76 eV, 6.44 eV respectively. According to these parameters, the chemical reactivity varies with the substituents of schiff bases. Nonlinear properties of *N*-(2,6-(4-dimethylaminobenzylidene)-*N′*-(2,4-dinitrophenyl) hydrazine is also confirmed by contour optimized structure shown in Fig. 4.

3.5 Mulliken charges distribution

The Mulliken charge distribution of all atoms of the optimized structure of the substituted Schiff base derivatives are calculated at the same level of theory. Mulliken charges for compound **4c** shown in Fig. 5.

The calculated results demonstrate that the atomic electronegativity plays vital roles for Mulliken charge distribution. The atom having bigger electronegativity will carry large negative charges, whereas the atom having smaller electronegativity will carry less negative or positive charges in the bonding between two atoms. So, for the studied compound N (from nitro group) are less negative, H and C (non-bonding with H atoms) are all positive. N (from amine group), O and C (bonding with H atoms) are all negative. Similar results are observed for other derivatives.

4 Experimental section

All materials otherwise noted were used as purchased without further purification. UV-visible spectra of the sample were recorded on UV-180 SHIMADZU Spectrophotometer with a scanning range of 800–220 nm. FTIR spectrum was recorded on IRTracer-100, SHIMADZU, Japan over the frequency range from 4000 to 400 cm^{-1} using KBr pellets. Melting point was measured by Stuart's electro thermal melting point apparatus (Model no.

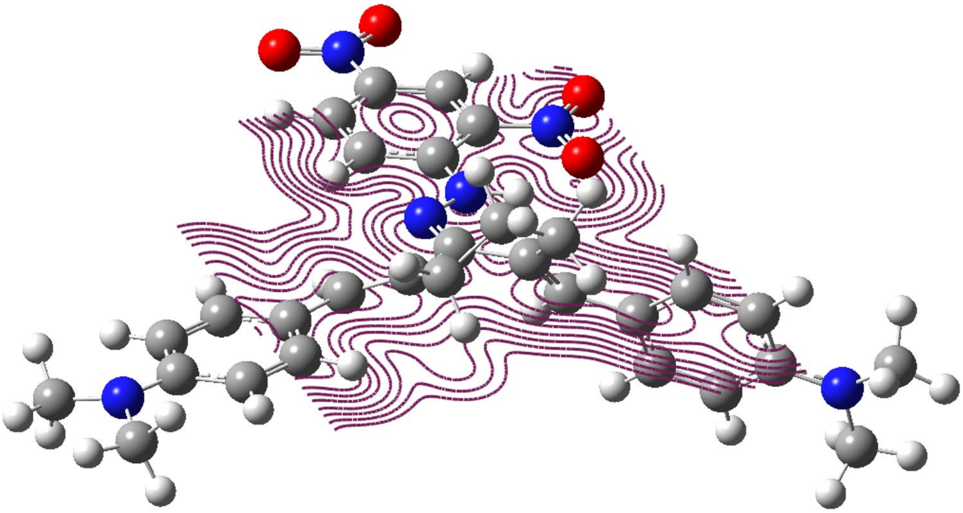

Fig. 4 Contour structure of *N*-(2,6-(4-dimethylaminobenzylidene)-*N′*-(2,4-dinitrophenyl)hydrazine at DFT B3LYP/6-311G+(2d,p) level of theory

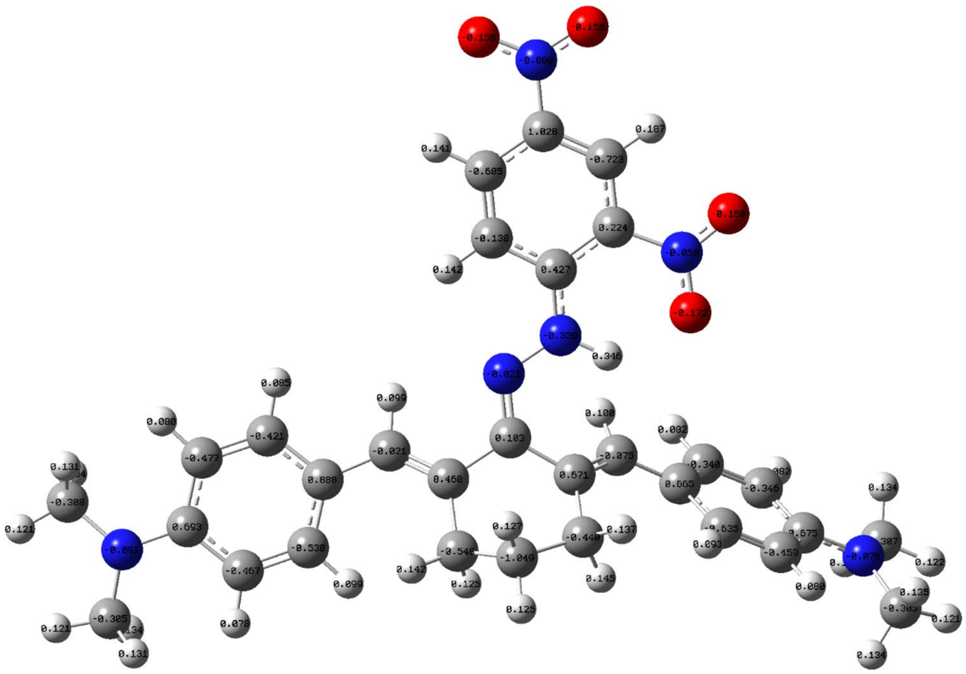

Fig. 5 Mulliken charges of *N*-(2,6-(4-dimethylaminobenzylidene)-*N′*-(2,4-dinitrophenyl)hydrazine at DFT B3LYP/6-311G+(2d,p) level of theory

SMP 30). ^{1}H NMR and ^{13}C NMR spectra of the sample were measured with an AVANCE Bruker NMR spectrometer at 400 MHz using suitable solvent and TMS as an internal standard. The elemental analysis was performed using CE-440 elemental analyzer, Exeter Analytical, Inc.

4.1 General procedure for synthesis of substituted bis-chalcones [27]

A mixture of cyclohexanone (1.0 equivalent), substituted benzaldehyde (2.0 equivalent), and sodium hydroxide pellet (2.2 equivalent) grinded in a mortar and pestle for 20 min at room temperature and then 10% hydrochloric acid was poured in the reaction mixture. The solid product was filtered and dried. The crude product was purified by recrystallization from ethanol and ethyl acetate.

4.1.1 2,6-Bis-(4-chlorobenzylidene)cyclohexanone (3a)

Yellowish green powder, m.p.: 127 °C, yield 90%. UV (EtOH): $\lambda_{max} = 336$. IR (KBr): 2929, 1666, 1575, 1576, 1489, 1263, 1159, 819, 798 cm^{-1}. ^{1}H NMR (400 MHz, CDCl$_3$) $\delta = 7.73$ (s, 2H, 2CH) 7.38–7.25 (m, 8H, Ar), 2.91–2.87 (m, 4H, 2CH$_2$), 1.84–1.77 (m, 2H, CH$_2$).

4.1.2 2,6-Bis-(4-methoxybenzylidene)cycloexanone (3b)

Pale yellow powder, m.p.: 152 °C, yield 88%. UV (EtOH): $\lambda_{max} = 360$. IR (KBr): 2937, 1656, 1593, 1161, 1184, 833 cm^{-1}. ^{1}H NMR (400 MHz, CDCl$_3$) $\delta = 7.76$ (s, 2H, 2CH), 7.45 (d, $J = 8.7$ Hz, 4H, Ar), 6.93 (d, $J = 8.7$ Hz, 4H, Ar), 3.85 (s, 6H, 2CH$_3$O), 2.92 (t, $J = 14.2$, 4H, 2CH$_2$), 1.84–1.78 (m, 2H, CH$_2$).

4.1.3 2,6-Bis-(4-dimethylaminobenzylidene) cyclohexanone (3c)

Yellow powder, m.p.: 136 °C, yield 85%. UV (EtOH): $\lambda_{max} = 450$. IR (KBr): 2915, 2853, 1658, 1551, 1367, 1302, 1159, 823 cm^{-1}. ^{1}H NMR (400 MHz, CDCl$_3$) $\delta = 7.76$ (s, 2H, 2CH), 7.45 (d, $J = 8.8$ Hz, 4H, Ar), 6.71 (d, $J = 8.8$ Hz, 4H, Ar), 3.01 (s, 12H, 2N(CH$_3$)$_2$), 2.94 (t, $J = 14.1$, 4H, 2CH$_2$), 1.83–1.79 (m, 2H, CH$_2$).

4.2 General procedure for synthesis of *N*-[2,6-bis-(benzylidene)cyclohexylidene]-*N′*-(2,4-dinitrophenyl)hydrazine derivatives [28]

2,4-dinitrophenyl hydrazine (1.0 mmol) and 20 mL of methanol were taken in a round bottom flask. Then 1.0 mL of 10% hydrochloric acid was added to this solution. After that substituted 2,6-bis-benzylidinecyclohexanone (1.0 mmol) was added to this clear solution. The reaction mixture was reflux for 2 h and allowed to stand for overnight. The residue was separated by filtration and washed with ethanol then dried in air. The crude product was separated by column chromatography.

4.2.1 N-[2,6-bis-(4-chlorobenzylidene)cyclohexanone]-N′-(2,4-dinitrophenyl)hydrazine (**4a**)

Flash column chromatography on silica gel using eluent (HX/EtOAc = 9/1; *v*/v). Red powder, m.p.: 185 °C, yield 83%. UV (EtOH): $\lambda_{max} = 342$. IR (KBr): 3263, 3095, 2941, 2916, 1612, 1585, 1508, 1490, 1332, 1139, 1082, 1055, 1010, 885, 827, 740, 653, 626 cm^{-1}. ^1H NMR (400 MHz, DMSO-d_6) δ: = 11.5 (s, 1H, N–H), 8.9 (d, *J* = 8.7 Hz, 1H, Ar), 8.5 (d, *J* = 8.7 Hz, 1H, Ar), 8.2 (d, *J* = 8.7 Hz, 1H, Ar), 7.5–7.4 (m, 8H, Ar), 7.2 (s, 2H, 2CH), 2.6–2.8 (m, 4H, cyclic), 1.7 (m, 2H, cyclic). ^{13}C NMR (125 MHz, DMSO-d_6): δ = 151, 143, 137, 134, 134, 133.5, 132, 129, 28, and 22. Anal. calcd for $C_{26}H_{20}Cl_2N_4O_4$ (523.37): C, 59.57; H, 3.81; N, 10.64; O, 12.18. Found C, 59.67; H, 3.85; N, 10.71; O, 12.23.

4.2.2 N-[2,6-bis-(4-methoxybenzylidene)cyclohexanone]-N′-(2,4-dinitrophenyl)hydrazine (**4b**)

Flash column chromatography on silica gel using eluent (HX/EtOAc = 9/1; *v*/v). Coffee color powder, m.p.: 225 °C, yield 65%. UV (EtOH): $\lambda_{max} = 384$. IR (KBr): 3269, 3107, 2931, 2835, 1612, 1585, 1506, 1475, 1249, 1170, 1130, 1076, 1024, 831, 740, 628 cm^{-1}. ^1H NMR (400 MHz, DMSO-d_6) δ: = 11.5 (s, 1H, N–H), 8.4 (d, *J* = 8.7 Hz, 1H, Ar), 8.0–8.1 (m, 4H, Ar), 7.7 (s, 1H, Ar), 7.2 (s, 1H, Ar) 7.0–7.1 (m, 4H, Ar), 6.9 (s, 2H, 2CH), 3.8 (s, 6H, $2CH_3O$), 1.6–1.8 (m, 4H, cyclic), 1.2 (m, 2H, cyclic). ^{13}C NMR (125 MHz, DMSO-d_6): δ = 150, 145, 137, 131.5, 130, 129, 127, 123, 117, 114, and 57. Anal. calcd for $C_{28}H_{26}N_4O_6$ (514.53): C, 65.31; H, 5.04; N, 10.81; O, 18.60. Found C, 65.36; H, 5.09; N, 10.89; O, 18.66.

4.2.3 N-[2,6-bis-(4-dimethylaminobenzylidene)cyclohexanone]-N′-(2,4-dinitrophenyl)hydrazine (**4c**)

Flash column chromatography on silica gel using eluent (HX/EtOAc = 9/1; *v*/v). Black powder, m.p.: 245 °C, yield 75%. UV (EtOH): $\lambda_{max} = 439$. IR (KBr): 3271, 3091, 2931, 2835, 1612, 1602, 1502, 1413, 1327, 1305, 1249, 1076, 1024, 829, 740, 628 cm^{-1}. ^1H NMR (400 MHz, DMSO-d_6): δ = 11.5 (s, 1H, N–H), 8.8 (s, 1H, Ar), 8.6 (s, 1H, Ar), 8.3–8.4 (m, 1H, Ar), 8.1 (d, *J* = 8.7 Hz, 4H, Ar), 7.8 (d, *J* = 8.7 Hz, 4H, Ar), 6.8 (s, 2H, 2CH), 3 (s, 12H, $4CH_3$), 2 (s, 4H, cyclic), 1.27 (s, 2H, cyclic). ^{13}C NMR (125 MHz, DMSO-d_6): δ = 151, 144, 136.5, 130, 129, 128.5, 123.5, 121, 116.5, and 112. Anal. calcd for $C_{30}H_{32}N_6O_4$ (540.61): C, 66.59; H, 5.92; N, 15.51; O, 11.79. Found C, 66.65; H, 5.97; N, 15.55; O, 11.84.

5 Computational method

Theoretical calculations were carried out using the Gaussain 16 program suite [29]. The geometries was entirely optimized by the DFT-B3LYP/6-311G+(2d,p) level of theory. Vibrational normal-mode analyses were performed at the same level to ensure that each optimized structure was a true minimum on the potential energy surface. Unscaled B3LYP/6-311G+(2d,p) frequencies were used to obtain thermochemical quantities, the thermal enthalpy and free energy corrections. After optimizations, the Mulliken charge and properties of frontier molecular orbitals of the studied compounds were investigated using the results calculated at B3LYP/6-311G+(2d,p) level of theory.

6 Conclusions

Hydrazone schiff base derivatives were synthesized in a general method for the addition of 2,4-dinitrophenylhydrazine and substituted 2,6-dibenzylidenecyclohexanone based bis-chalcones in the presence of acid. The characteristics signal for the proton of NH, the δ value 11.5 ppm in ^1H NMR and signals are for azomethine carbon between δ from 143 and 150 ppm in ^{13}C NMR spectra were observed. Theoretical studies were performed by DFT method using B3LYP/6-311G+(2d,p) level of theory. Nonlinear structure of the compounds were found through optimizing the structure. The energy of HOMO and LUMO molecular orbital showed the possibility of intramolecular charge transfer as well as hydrogen bond. Quantum chemical parameters of compounds were estimated using E_{HOMO} and E_{LUMO}. It was found that chemical potential (μ) and electronegativity (χ); chemical hardness (η) and electrophilicity (ω) follow the order **4a** > **4b** > **4c** whereas chemical softness (σ) and nucleophilicity (ε) follow the reverse order **4a** < **4b** < **4c**. The results revealed that substituent effect plays a vital role on stability, reactivity and excitation of the compounds.

Acknowledgements The authors are acknowledging Khulna University of Engineering & Technology for financial support and necessary facilities. The authors are also grateful to Prof. Dr. Manabu Abe, Graduate School of Advanced Science and Engineering, Hiroshima University, Japan, for supporting the NMR analysis.

Compliance with ethical standards

Conflict of interest The authors declare that they have no conflict of interest.

References

1. Schiff H (1869) Untersuchungen über Salicinderivate. Justus Liebigs Ann Chem 150:193–200. https://doi.org/10.1002/jlac.18691500206
2. Lygaitis R, Getautis V, Grazulevicius JV (2008) Hole-transporting hydrazones. Chem Soc Rev 37:770–788. https://doi.org/10.1039/b702406c
3. Kucukoglu K, Gul HI, Taslimi P, Gulcin I, Supuran CT (2019) Investigation of inhibitory properties of some hydrazone compounds on hCA I, hCA II and AChE enzymes. Bioorg Chem 86:316–321. https://doi.org/10.1016/j.bioorg.2019.02.008
4. Patra D, Paul S, Sepay N, Kundu R, Ghosh T (2018) Structure-activity relationship on DNA binding and anticancer activities of a family of mixed-ligand oxidovanadium (V) hydrazone complexes. J Biomol Struct Dyn 36:4143–4155. https://doi.org/10.1080/07391102.2017.1409652
5. Al Zoubi W, Al-Hamdani AAS, Ahmed SD, Ko YG (2018) A new azo-Schiff base: synthesis, characterization, biological activity and theoretical studies of its complexes. Appl Organomet Chem 32:3895. https://doi.org/10.1002/aoc.3895
6. Wang X, Yin J, Shi L, Zhang G, Song B (2014) Design, synthesis, and antibacterial activity of novel Schiff base derivatives of quinazolin-4(3H)-one. Eur J Med Chem 77:65–74. https://doi.org/10.1016/j.ejmech.2014.02.053
7. Mukherjee AJ, Zade SS, Singh HB, Sunoj RB (2010) Organoselenium chemistry: role of intramolecular interactions. Chem Rev 110:4357–4416. https://doi.org/10.1021/cr900352j
8. Al Zoubi W, Ko YG (2017) Schiff base complexes and their versatile applications as catalysts in oxidation of organic compounds: Part I. Appl Organomet Chem 31:3574. https://doi.org/10.1002/aoc.3574
9. Radunsky C, Kösters J, Müller J (2015) Chromogenic behaviour of a family of hydrazine and hydrazone metal complexes. Inorg Chim Acta 428:14–20. https://doi.org/10.1016/j.ica.2015.01.012
10. Fekri R, Salehi M, Asadi A, Kubicki M (2019) Synthesis, characterization, anticancer and antibacterial evaluation of Schiff base ligands derived from hydrazone and their transition metal complexes. Inorg Chim Acta 484:245–254. https://doi.org/10.1016/j.ica.2018.09.022
11. Malik MA, Dar OA, Gull P, Wani MY, Hashmi AA (2018) Heterocyclic Schiff base transition metal complexes in antimicrobial and anticancer chemotherapy. MedChemComm 9:409–436. https://doi.org/10.1039/c7md00526a
12. Zhang JP, Zhang YB, Lin JB, Chen XM (2012) Metal azolate frameworks: from crystal engineering to functional materials. Chem Rev 112:1001–1033. https://doi.org/10.1021/cr200139g
13. Al Zoubi W, Al Mohanna N (2014) Membrane sensors based on Schiff bases as chelating ionophores–a review. Spectrochim Acta A 132:854–870
14. Jasinski JP, Braley AN, Chidan Kumar CS et al (2011) (E)-1-(2,4-Dinitrophenyl)-2-(2-fluorobenzylidene) hydrazine. Acta Crystallogr E 67:1200–1201. https://doi.org/10.1107/S1600536811014383
15. Kaya Y, Yilmaz VT, Buyukgungor O (2016) Synthesis, spectroscopic, structural and quantum chemical studies of a new imine oxime and its palladium(II) complex: hydrolysis mechanism. Molecules 21:52. https://doi.org/10.3390/molecules21010052
16. Basavarajappa KV, Arthoba Nayaka Y, Purushothama HT et al (2020) Optical, electrochemical and current–voltage characteristics of novel coumarin based 2,4-dinitrophenylhydrazone derivatives. J Mol Struct 1199:126946. https://doi.org/10.1016/j.molstruc.2019.126946
17. Suydam FH (1963) The C=N stretching frequency in azomethines. Anal Chem 35:193–195. https://doi.org/10.1021/ac60195a024
18. Hussain MM, Rahman MM, Arshad MN, Asiri AM (2017) Hg^{2+} sensor development based on (E)-N′-nitrobenzylidene-benzenesulfonohydrazide (NBBSH) derivatives fabricated on a glassy carbon electrode with a Nafion matrix. ACS Omega 2:420–431. https://doi.org/10.1021/acsomega.6b00359
19. Feilchenfeld H (1959) A relation between the lengths of single, double and triple bonds. J Phys Chem 63:1346. https://doi.org/10.1021/j150578a603
20. Mary YS, Raju K, Yildiz I et al (2012) FT-IR, FT-Raman, SERS and computational study of 5-ethylsulphonyl-2-(o-chlorobenzyl) benzoxazole. Spectrochim Acta A 96:617–625. https://doi.org/10.1016/j.saa.2012.07.006
21. Merrick JP, Moran D, Radom L (2007) An evaluation of harmonic vibrational frequency scale factors. J Phys Chem A 111:11683–11700. https://doi.org/10.1021/jp073974n
22. Kumar A, Srivastava AK, Gangwar S, Misra N, Mondal A, Brahmachari G (2015) Combined experimental (FT-IR, UV-visible spectra, NMR) and theoretical studies on the molecular structure, vibrational spectra, HOMO, LUMO, MESP surfaces, reactivity descriptor and molecular docking of Phomarin. J Mol Struct 1096:94–101. https://doi.org/10.1016/j.molstruc.2015.04.031
23. Kafer D, El Helou M, Gemel C, Witte G (2008) Packing of planar organic molecules: interplay of van der Waals and electrostatic interaction. Cryst Growth Des 8:3053–3057. https://doi.org/10.1021/cg800195u
24. Parr RG, Pearson RG (1983) Absolute hardness: companion parameter to absolute electronegativity. J Am Chem Soc 105:7512–7516. https://doi.org/10.1021/ja00364a005
25. Nitti A, Signorile M, Boiocchi M et al (2016) Conjugated thiophene-fused isatin dyes through intramolecular direct arylation. J Org Chem 81:11035–11042. https://doi.org/10.1021/acs.joc.6b01922
26. Pearson RG (1989) Absolute electronegativity and hardness: applications to organic chemistry. J Org Chem 54:1423–1430. https://doi.org/10.1021/jo00267a034
27. Badal MMR, Ashekul Islam HM, Maniruzzaman M, Abu Yousuf M (2020) Acidochromic behavior of dibenzylidene cyclohexanone-based bischalcone: experimental and theoretical study. ACS Omega 5:22978–22983. https://doi.org/10.1021/acsomega.0c02556
28. Behforouz M, Flynt MS, Bolan JL (1985) 2,4-Dinitrophenylhydrazones: a modified method for the preparation of these derivatives and an explanation of previous conflicting results. J Org Chem 50:1186–1189. https://doi.org/10.1021/jo00208a009
29. Frisch MJ, Trucks GW, Schlegel HB et al (2016) Gaussian 16 Revision C01. Gaussian Inc, Wallingford CT